

Lepton-Flavour Violation in Supersymmetric Models with Trilinear R-parity Violation

André de Gouvêa, Smaragda Lola, and Kazuhiro Tobe

*CERN – Theory Division
CH-1211 Genève 23, Switzerland*

Abstract

Supersymmetry with R-parity violation (RPV) provides an interesting framework for naturally accommodating small neutrino masses. Within this framework, we discuss the lepton-flavour violating (LFV) processes $\mu \rightarrow e\gamma$, $\mu \rightarrow eee$, and $\mu \rightarrow e$ conversion in nuclei. We make a detailed study of the observables related to LFV in different RPV models, and compare them to the expectations of R-conserving supersymmetry with heavy right-handed neutrinos. We show that the predictions are vastly different and uniquely characterise each model, thus providing a powerful framework for experimentally distinguishing between different theories of LFV. Besides the obvious possibility of amplified tree-level generation of $\mu \rightarrow eee$ and $\mu \rightarrow e$ conversion in nuclei, we find that even in the case where these processes arise at the one-loop level, their rates are comparable to that of $\mu \rightarrow e\gamma$, in clear contrast to the predictions of R-conserving models. We conclude that in order to distinguish between the different models, such a combined study of *all* the LFV processes is necessary, and that measuring P-odd asymmetries in polarised $\mu \rightarrow eee$ can play a decisive role. We also comment on the intriguing possibility of RPV models yielding a large T-odd asymmetry in the decay of polarised $\mu \rightarrow eee$.

1 Introduction

Recently, neutrino oscillation experiments [1, 2, 3] have provided very strong evidence for non-zero, yet tiny, neutrino masses. In order to accommodate such small masses, it is widely believed that new physics beyond the Standard Model (SM) is required. One of the simplest and most elegant mechanisms for generating a small neutrino mass is to introduce extra standard model singlets to the SM Lagrangian, and allow them to acquire a very large Majorana mass (this is the well known seesaw mechanism [4]). There are many important phenomenological consequences of neutrino masses. One of them is that individual lepton-flavour numbers are not conserved, which implies that SM forbidden processes such as $\mu \rightarrow e\gamma$ may occur. However, given the size of the neutrino masses, the rates for charged lepton flavour violating (LFV) phenomena are extremely small in the SM plus massive neutrinos [5].

There are other hints for physics beyond the SM, including the gauge hierarchy problem. Low-energy supersymmetry (SUSY) is one of the preferred candidates for beyond the SM physics which solves the hierarchy problem. SUSY models can easily accommodate the seesaw mechanism, and SUSY even helps in the sense that it stabilises the (very heavy) Majorana mass of the right-handed neutrino. Furthermore, in such a framework, LFV processes in the charged lepton sector such as $\mu \rightarrow e\gamma$, $\mu \rightarrow eee$, and $\mu \rightarrow e$ conversion in nuclei are potentially amplified, as has been previously discussed [6, 7, 8, 9], and the rates for such processes can be within the reach of future experiments. The reason for this is that while in the SM plus massive neutrinos the amplitudes for LFV violation are proportional to the neutrino masses (*i.e.*, suppressed by the very large right-handed neutrino masses, in the case of the seesaw mechanism), in SUSY models these processes are only suppressed by inverse powers of the supersymmetry breaking scale, which is at most $O(1)$ TeV.

Another SM extension which naturally accommodates non-zero neutrino masses is SUSY with R-parity violation (RPV). R-parity is usually imposed as a global symmetry of the minimal supersymmetric version of the SM (MSSM) in order to prevent an unacceptably large rate for proton decay. However, this proves to be somewhat of an overkill, since R-parity conservation implies both baryon number and lepton number conservation, while to stop proton decay only one or the other needs to be exactly conserved. In light of the evidence for neutrino masses, which can potentially be Ma-

Majorana particles and therefore violate lepton number, one may, instead, take advantage of RPV operators to generate small neutrino masses.

In this paper, we consider SUSY models with RPV but with baryon parity (in order to satisfy the current experimental upper limits on the proton lifetime [10]).¹ These models naturally generate small Majorana neutrino masses, if the RPV couplings are small [13, 14, 15].² In such RPV models, “large” LFV in the charged lepton sector is also generically expected. Indeed, as has been pointed out in the literature [17, 18, 19, 20, 21, 22], the most stringent limits on certain products of RPV couplings come from the present experimental bounds on charged LFV processes. Therefore it is important to understand some of the general features of LFV in models with RPV.

It is interesting to consider how searches for LFV at low energy experiments compare to those at colliders. For instance, the simultaneous presence of R-violating operators that couple both to $e - q$ and to $\mu - q$ ($\tau - q$) pairs, would lead to $\mu + \text{jet}$ ($\tau + \text{jet}$) final states at HERA [23]. It turns out that for $e \leftrightarrow \tau$ transitions, the high energy experimental probes provide the strongest bounds, while for $e \leftrightarrow \mu$ transitions stopped muon experiments provide, by far, the most stringent bounds. Finally, the strongest bound for $\tau \leftrightarrow \mu$ transitions comes from $\tau \rightarrow \mu\gamma$ searches at CLEO [24] ($Br(\tau \rightarrow \mu\gamma) < 1.1 \times 10^{-6}$) which is less restrictive. In the near future, the experimental sensitivity to some rare muon processes is going to improve by two to three orders of magnitude, while a similar improvement is not expected for other LFV processes. For this reason, we will focus on processes with stopped muons, which not only provide the stringest quantitative bounds on LFV today, but which will be significantly probed in the near future.

In this paper, we discuss the LFV processes $\mu^+ \rightarrow e^+\gamma$, $\mu^+ \rightarrow e^+e^-e^+$, and $\mu^- \rightarrow e^-$ conversion in the case of models with trilinear RPV. In Sec. 2, we briefly introduce the SUSY models with trilinear RPV which will be considered here. In Sec. 3, we present the formalism for computing branching ratios and asymmetries of the relevant LFV processes. In Sec. 4, we consider LFV processes in some representative cases, including those in which the branching ratio for $\mu^+ \rightarrow e^+\gamma$ is much smaller than the branching ratio for

¹In cosmology, large RPV Yukawa couplings may erase a pre-existing baryon asymmetry [11]. Here we do not consider such constraints since they are model-dependent and can be evaded in several baryogenesis scenarios [12].

²A mechanism which explains why RPV couplings are small is required. This can be achieved, for example, by imposing flavour symmetries which relate the lepton and baryon number violating Yukawa couplings to those that generate fermion masses [16].

$\mu^+ \rightarrow e^+e^-e^+$ and/or the rate for $\mu^- \rightarrow e^-$ conversion in nuclei, which can be generated at the tree-level. Even if all LFV processes occur at the one-loop level, the rates for all three processes considered here are comparable. These features are completely different from the predictions of other neutrino mass generating SUSY frameworks, such as the MSSM with right-handed neutrinos [7]. In the latter, the branching ratio for $\mu^+ \rightarrow e^+\gamma$ is much larger than that for $\mu^+ \rightarrow e^+e^-e^+$ and the rate for $\mu^- \rightarrow e^-$ conversion in nuclei, even though all processes are also generated at the one-loop level. We also show that P-odd asymmetries in the $\mu^+ \rightarrow e^+e^-e^+$ process (which require polarised muons in order to be measured) are very useful in order to distinguish different models. Sec. 5 contains our conclusions. In Appendix A we provide explicit expressions for the LFV vertices in the case of models with RPV, while in Appendix B we discuss the current bounds on certain pairs of RPV couplings from LFV processes and comment on neutrino masses.

2 SUSY models with trilinear R-parity violation

Here, we briefly introduce the SUSY models with RPV which will be discussed in the upcoming sections. If R-parity conservation is not postulated, in addition to ordinary Yukawa interactions, the following terms are allowed in the MSSM superpotential:

$$W_{RPV} = \frac{\lambda_{ijk}}{2} L_i L_j \bar{E}_k + \lambda'_{ijk} L_i Q_j \bar{D}_k + \lambda''_{ijk} \bar{U}_i \bar{D}_j \bar{D}_k + \mu'_i L_i H_u, \quad (2.1)$$

where L_i , \bar{E}_i , Q_i , \bar{U}_i , \bar{D}_i , and H_u denote the left-handed doublet lepton, right-handed lepton, left-handed doublet quark, right-handed up-type quark, right-handed down-type quark, and “up-type” Higgs superfields, respectively. The indices i, j and k range from 1 to 3 for different quark/lepton flavours. Throughout this paper, in order to forbid rapid proton decay, we impose baryon parity [10], so all λ'' couplings are zero. We also make the simplifying assumption that all μ' also vanish.³ In light of these assumptions, the superpotential above yields the following Lagrangian:

$$\mathcal{L} = \lambda_{ijk} (\bar{\nu}_{Li}^c e_{Lj} \tilde{e}_{Rk}^* + \bar{e}_{Rk} \nu_{Li} \tilde{e}_{Lj} + \bar{e}_{Rk} e_{Lj} \tilde{\nu}_{Li})$$

³Even if μ'_i were non-zero, their contributions to LFV processes would be, in general, negligible because of neutrino mass constraints [14, 22].

$$\begin{aligned}
& + \lambda'_{ijk} V_{KM}^{j\alpha} \left(\bar{\nu}_{Li}^c d_{L\alpha} \tilde{d}_{Rk}^* + \bar{d}_{Rk} \nu_{Li} \tilde{d}_{L\alpha} + \bar{d}_{Rk} d_{L\alpha} \tilde{\nu}_{Li} \right) \\
& - \lambda'_{ijk} \left(\bar{u}_j^c e_{Li} \tilde{d}_{Rk}^* + \bar{d}_{Rk} e_{Li} \tilde{u}_{Lj} + \bar{d}_{Rk} u_{Lj} \tilde{e}_{Li} \right) + \text{h.c.}, \quad (2.2)
\end{aligned}$$

where f ($f = \nu, e, d$, and u) denotes fermions and \tilde{f} sfermions, and the index (R, L) indicates the field's chirality. We assume that the RPV Yukawa couplings above (λ_{ijk} and λ'_{ijk}) are the only source of LFV. In what follows, Eq. (2.2) is what is referred to by ‘‘RPV model.’’

3 Branching ratios and asymmetries for the LFV processes

In this section, we present complete expressions for the branching ratios for the LFV processes $\mu^+ \rightarrow e^+ \gamma$, $\mu^+ \rightarrow e^+ e^- e^+$, and $\mu^- \rightarrow e^-$ conversion in nuclei, for the P-odd asymmetry in $\mu^+ \rightarrow e^+ \gamma$, and for the P-odd and T-odd asymmetries in $\mu^+ \rightarrow e^+ e^- e^+$.

3.1 $\mu^+ \rightarrow e^+ \gamma$

The process $\mu^+ \rightarrow e^+ \gamma^{(*)}$ is generated by photon penguin diagrams (see the penguin diagrams in Figs. 1, 2, and 4). The amplitude for this process can be written as follows:

$$\begin{aligned}
T = e\epsilon^{\alpha*} \bar{v}_\mu(p) & \left[(A_1^L P_L + A_1^R P_R) \gamma^\beta (g_{\alpha\beta} q^2 - q_\alpha q_\beta) \right. \\
& \left. + m_\mu i \sigma_{\alpha\beta} q^\beta (A_2^L P_L + A_2^R P_R) \right] v_e(p - q) \quad (3.1)
\end{aligned}$$

where $v_{\mu(e)}$ and ϵ are the antimuon (positron) and photon wave functions, and p and q are the antimuon and photon momenta, respectively. P_L and P_R are chirality projection operators: $P_L = (1 - \gamma_5)/2$, and $P_R = (1 + \gamma_5)/2$, while $\sigma_{\alpha\beta} = (i/2)[\gamma_\alpha, \gamma_\beta]$. The effective couplings $A_1^{L,R}$ come from off-shell photon diagrams ($q^2 \neq 0$), which only contribute to $\mu^+ \rightarrow e^+ e^- e^+$ and $\mu \rightarrow e$ conversion in nuclei. On the other hand, the couplings $A_2^{L,R}$ arise from the on-shell photon diagrams ($q^2 = 0$), which induce $\mu^+ \rightarrow e^+ \gamma$ as well as $\mu^+ \rightarrow e^+ e^- e^+$ and $\mu^- \rightarrow e^-$ conversion in nuclei. Explicit expressions for $A_{1,2}^{L,R}$ in models with RPV are presented in Appendix A.

In the $\mu^+ \rightarrow e^+ \gamma$ decay, it has been argued [25] that a nonzero muon polarisation is useful not only to suppress background processes, but also to

distinguish between $\mu^+ \rightarrow e_L^+ \gamma$ and $\mu^+ \rightarrow e_R^+ \gamma$. The differential branching ratio for $\mu^+ \rightarrow e^+ \gamma$ is given by

$$\frac{d\text{Br}(\mu^+ \rightarrow e^+ \gamma)}{d \cos \theta} = \frac{\text{Br}(\mu^+ \rightarrow e^+ \gamma)}{2} \{1 + A_P P \cos \theta\}, \quad (3.2)$$

where P is the muon polarisation and θ is the angle between the positron momentum and the polarisation direction. Here, the branching ratio $\text{Br}(\mu^+ \rightarrow e^+ \gamma)$ and the P-odd asymmetry A_P are

$$\text{Br}(\mu^+ \rightarrow e^+ \gamma) = \frac{48\pi^3 \alpha}{G_F^2} (|A_2^L|^2 + |A_2^R|^2), \quad (3.3)$$

$$A_P = \frac{|A_2^L|^2 - |A_2^R|^2}{|A_2^L|^2 + |A_2^R|^2}, \quad (3.4)$$

where G_F is the Fermi constant, and α is the fine-structure constant.

3.2 Polarised $\mu^+ \rightarrow e^+ e^+ e^-$

In the RPV models, some of the $LL\bar{E}$ couplings (λ_{ijk}) generate $\mu^+ \rightarrow e^+ e^- e^+$ at tree-level (Fig. 1), while the photon penguin vertices $A_{1,2}^{L,R}$ also contribute.⁴ The amplitude for $\mu^+ \rightarrow e^+ e^- e^+$ is

$$\begin{aligned} T = & B^L \bar{v}_\mu(p) P_L \gamma_\mu v_e(p_2) \bar{u}_e(p_3) P_R \gamma^\mu v_e(p_1) \\ & + B^R \bar{v}_\mu(p) P_R \gamma_\mu v_e(p_2) \bar{u}_e(p_3) P_L \gamma^\mu v_e(p_1) \\ & + 4\pi\alpha \bar{v}_\mu(p) \left\{ (A_1^L P_L + A_1^R P_R) \gamma_\mu + m_\mu i \frac{\sigma_{\mu\nu} q^\nu}{q^2} (A_2^R P_R + A_2^L P_L) \right\} v_e(p_2) \\ & \times \bar{u}_e(p_3) \gamma^\mu v_e(p_1) - (p_1 \leftrightarrow p_2), \end{aligned} \quad (3.5)$$

where the explicit expressions for the tree-level vertices $B^{R(L)}$ in models with RPV are given in Appendix A.

When the muon is polarised, two P-odd and one T-odd asymmetry can be defined [26, 27]. Using the notation introduced by Okada *et al.* [27], the z -axis is taken to be the direction of the electron momentum and the $(z \times x)$ -plane is taken to be the decay plane. The positron with the largest energy

⁴There is also a Z-penguin contribution. However, its contribution is suppressed by m_f^2/m_Z^2 where m_f is the typical fermion mass in the process. Therefore we simply neglect it. In order to be consistent, we will not study processes where top-quarks are involved.

is denoted as positron 1 and the other as positron 2. The x -coordinate is defined as $(p_1)_x \geq 0$ where \vec{p}_1 is the momentum of positron 1. It is in this coordinate system that the direction of the muon polarisation \vec{P} , used below, is defined. (For details, see [27].) Finally, the P-odd and T-odd asymmetries are defined as follows:

$$\begin{aligned} A_{P_1} &= \frac{N(P_z > 0) - N(P_z < 0)}{N(P_z > 0) + N(P_z < 0)}, \\ &= \frac{3}{2\text{Br}(\delta)} \{0.61(C_1 - C_2) - 0.12(C_3 - C_4) + 5.6(C_5 - C_6) \\ &\quad - 4.7(C_7 - C_8) + 2.5(C_9 - C_{10})\}, \end{aligned} \quad (3.6)$$

$$\begin{aligned} A_{P_2} &= \frac{N(P_x > 0) - N(P_x < 0)}{N(P_x > 0) + N(P_x < 0)}, \\ &= \frac{3}{2\text{Br}(\delta)} \{0.1(C_3 - C_4) + 10(C_5 - C_6) \\ &\quad + 2.0(C_7 - C_8) - 1.6(C_9 - C_{10})\}, \end{aligned} \quad (3.7)$$

$$\begin{aligned} A_T &= \frac{N(P_y > 0) - N(P_y < 0)}{N(P_y > 0) + N(P_y < 0)}, \\ &= \frac{3}{2\text{Br}(\delta)} \{2.0C_{11} - 1.6C_{12}\}, \end{aligned} \quad (3.8)$$

where the muons are assumed to be 100% polarised, and $N(P_i > (<)0)$ denotes the number of events with a positive (negative) P_i component for the muon polarisation. Here an energy cutoff for positron 1 is introduced ($E_1 < (m_\mu/2)(1 - \delta)$) and henceforth we will consider $\delta = 0.02$, following Okada *et al.* [27]. This choice is made in order to optimise the T-odd asymmetry. Of course, one can obtain more information concerning the C_i coefficients, including the CP-odd terms C_{11} and C_{12} , (see definition of C_i in what follows) by analysing the Dalitz plot of the $\mu^+ \rightarrow e^+e^-e^+$ decay. C_i ($i = 1 - 12$) are functions of the effective couplings $A_{1,2}^{L,R}$ and $B^{L,R}$:

$$C_1 = \frac{2\pi^2\alpha^2}{G_F^2}|A_1^R|^2, \quad C_2 = \frac{2\pi^2\alpha^2}{G_F^2}|A_1^L|^2, \quad (3.9)$$

$$C_3 = \frac{1}{8G_F^2}|B^R + 4\pi\alpha A_1^R|^2, \quad C_4 = \frac{1}{8G_F^2}|B^L + 4\pi\alpha A_1^L|^2, \quad (3.10)$$

$$C_5 = \frac{\pi^2\alpha^2}{2G_F^2}|A_2^R|^2, \quad C_6 = \frac{\pi^2\alpha^2}{2G_F^2}|A_2^L|^2, \quad (3.11)$$

$$C_7 = -\frac{\pi^2 \alpha^2}{G_F^2} \text{Re}(A_2^R A_1^{L*}), \quad C_8 = -\frac{\pi^2 \alpha^2}{G_F^2} \text{Re}(A_2^L A_1^{R*}), \quad (3.12)$$

$$C_9 = -\frac{\pi \alpha}{4G_F^2} \text{Re}\{A_2^R (B^{L*} + 4\pi \alpha A_1^{L*})\}, \quad (3.13)$$

$$C_{10} = -\frac{\pi \alpha}{4G_F^2} \text{Re}\{A_2^L (B^{R*} + 4\pi \alpha A_1^{R*})\}, \quad (3.14)$$

$$C_{11} = \frac{\pi \alpha}{8G_F^2} \text{Im}\{8\pi \alpha (A_2^R A_1^{L*} + A_2^L A_1^{R*})\}, \quad (3.15)$$

$$C_{12} = \frac{\pi \alpha}{4G_F^2} \text{Im}\{A_2^R (B^{L*} + 4\pi \alpha A_1^{L*}) + A_2^L (B^{R*} + 4\pi \alpha A_1^{R*})\}. \quad (3.16)$$

The branching ratio for $\delta = 0.02$ is

$$\begin{aligned} \text{Br}(\delta = 0.02) &= 1.8(C_1 + C_2) + 0.96(C_3 + C_4) + 88(C_5 + C_6) \\ &\quad + 14(C_7 + C_8) + 8(C_9 + C_{10}). \end{aligned} \quad (3.17)$$

The branching ratio for $\mu^+ \rightarrow e^+ e^- e^+$ for $\delta = 0$ is given by

$$\begin{aligned} \text{Br}(\mu^+ \rightarrow e^+ e^- e^+) &= 2(C_1 + C_2) + C_3 + C_4 + 32 \left\{ \log \frac{m_\mu^2}{m_e^2} - \frac{11}{4} \right\} (C_5 + C_6) \\ &\quad + 16(C_7 + C_8) + 8(C_9 + C_{10}) \\ &= \frac{1}{8G_F^2} \left[|B^L|^2 + |B^R|^2 + 48\pi^2 \alpha^2 \left\{ |A_1^L|^2 + |A_1^R|^2 \right. \right. \\ &\quad \left. \left. + \frac{8}{3} \left(\log \frac{m_\mu^2}{m_e^2} - \frac{11}{4} \right) (|A_2^R|^2 + |A_2^L|^2) - 4\text{Re}(A_1^L A_2^{R*} + A_1^R A_2^{L*}) \right\} \right. \\ &\quad \left. + 8\pi \alpha \text{Re}\{A_1^L B^{L*} + A_1^R B^{R*} - 2(A_2^R B^{L*} + A_2^L B^{R*})\} \right]. \end{aligned} \quad (3.18)$$

3.3 $\mu^- \rightarrow e^-$ conversion in nuclei

Similarly to $\mu^+ \rightarrow e^+ e^- e^+$, not only photon penguin diagrams but also tree-level diagram induced by some of the $LQ\bar{D}$ Yukawa couplings (λ'_{ijk}) can generate $\mu^- \rightarrow e^-$ conversion in nuclei. The amplitude is given by

$$\begin{aligned} T &= D^u \bar{u}_e \gamma_\mu P_L u_\mu \bar{u}_u \gamma_\mu P_L u_u + D^d \bar{u}_e \gamma_\mu P_L u_\mu \bar{u}_d \gamma_\mu P_R u_d \\ &\quad - 4\pi \alpha \bar{u}_e \left\{ \gamma_\mu (A_1^{L*} P_L + A_1^{R*} P_R) + m_\mu i \frac{\sigma_{\mu\nu} q^\nu}{q^2} (A_2^{R*} P_R + A_2^{L*} P_L) \right\} u_\mu \\ &\quad \times \sum_{q=u,d} Q_q \bar{u}_q \gamma_\mu u_q, \end{aligned} \quad (3.20)$$

where the complete expressions for the tree-level contributions $D^{u,d}$ in the case of RPV models are presented in Appendix A. The $\mu^- \rightarrow e^-$ conversion rate is

$$\begin{aligned} \text{R}(\mu^- \rightarrow e^-) &= \frac{\alpha^3 Z_{eff}^4 |F(q)|^2 m_\mu^5}{16\pi^2 Z \Gamma(\mu \text{ capture})} \left\{ 64\pi^2 \alpha^2 |A_1^R - A_2^L|^2 \right. \\ &\quad \left. + \left| (2Z + N)D^u + (Z + 2N)D^d - 8\pi\alpha Z(A_1^{L*} - A_2^{R*}) \right|^2 \right\}, \end{aligned} \quad (3.21)$$

where $\Gamma(\mu \text{ capture})$ is the muon capture rate in the nucleus of interest [28], Z and N are the proton and neutron numbers, respectively, $F(q)$ is the nuclear form factor as a function of the momentum transfer and Z_{eff} is the nuclear effective charge [29]. In some of the most commonly used nuclei, $^{48}_{22}\text{Ti}$ and $^{27}_{13}\text{Al}$, these nuclear parameters are given by [29]

$$\begin{aligned} \Gamma(\mu \text{ capture}) &= 2.590 \times 10^6 \text{ s}^{-1} = 1.7 \times 10^{-18} \text{ GeV}, \\ Z = 22, \quad Z_{eff} &= 17.61, \quad |F(q^2 = -m_\mu^2)| = 0.535 \quad \text{for } ^{48}_{22}\text{Ti}, \end{aligned} \quad (3.22)$$

and

$$\begin{aligned} \Gamma(\mu \text{ capture}) &= 0.7054 \times 10^6 \text{ s}^{-1} = 4.6 \times 10^{-19} \text{ GeV}, \\ Z = 13, \quad Z_{eff} &= 11.62, \quad |F(q^2 = -m_\mu^2)| = 0.64 \quad \text{for } ^{27}_{13}\text{Al}. \end{aligned} \quad (3.23)$$

4 LFV in representative cases

The most severe constraints on some particular products of trilinear RPV couplings come from the present experimental upper limits on the branching ratios of the LFV processes discussed in the previous section (see Appendix B) [17, 18, 19, 20, 21, 22]. Therefore, searches for LFV in muon processes are particularly sensitive to models with RPV. Generically, it is very hard to make definite predictions for the branching ratios of the LFV processes since the number of new Yukawa couplings ($\lambda_{ijk}, \lambda'_{ijk}$) is too large. Here we consider, instead, different cases where only a small number of RPV couplings is significant for LFV. This is done not only to simplify the problem at hand, but also to identify features of LFV which are not only different from those in the “traditional” models, such as the MSSM with heavy right-handed neutrinos discussed in [6, 7, 8], but which can also be used to characterise the different cases themselves. This dominance of specific RPV couplings is also a consequence of certain flavour models [16].

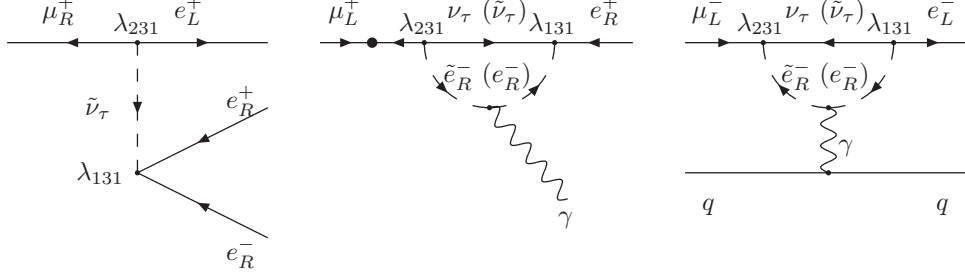


Figure 1: *Lowest order Feynman diagrams for lepton flavour violating processes induced by $\lambda_{131}\lambda_{231}$ couplings (see Eq. (2.1)).*

4.1 $\mu^+ \rightarrow e^+e^-e^+$ induced at tree-level

First, we consider a model in which only the Yukawa couplings λ_{131} and λ_{231} are non-zero. In this case, $\mu^+ \rightarrow e^+e^-e^+$ is generated at the tree-level, while the other LFV processes ($\mu^+ \rightarrow e^+\gamma$ and $\mu^- \rightarrow e^-$ conversion in nuclei) are induced via photon penguin diagrams at the one-loop level, as shown in Fig. 1.

The effective vertices are given by

$$B^L = -\frac{\lambda_{131}\lambda_{231}}{2m_{\tilde{\nu}_\tau}^2}, \quad (4.1)$$

$$A_2^R = -\frac{\lambda_{131}\lambda_{231}}{96\pi^2 m_{\tilde{\nu}_\tau}^2} \left(1 - \frac{m_{\tilde{\nu}_\tau}^2}{2m_{\tilde{e}_R}^2}\right), \quad (4.2)$$

$$A_1^L = \frac{\lambda_{131}\lambda_{231}}{96\pi^2 m_{\tilde{\nu}_\tau}^2} \left(-\frac{8}{3} - 2\log \frac{m_e^2}{m_{\tilde{\nu}_\tau}^2} + \frac{m_{\tilde{\nu}_\tau}^2}{3m_{\tilde{e}_R}^2} - 2\delta(m_e^2/q^2)\right). \quad (4.3)$$

Here we assume, without loss of generality, that the RPV couplings are real. The function δ is presented in Appendix A. In $\mu^- \rightarrow e^-$ conversion, we assume the momentum of the virtual photon to be $q^2 = -m_\mu^2$ in order to compute $\delta(m_e^2/q^2)$ in A_1^L , while in the case of $\mu^+ \rightarrow e^+e^-e^+$, we simply set $q^2 = 0$ ($\delta = 0$), since the tree-level contribution B^L is much larger than the contribution from $\delta(m_e^2/q^2)$. The ratios of branching ratios, $\text{Br}(\mu^+ \rightarrow e^+\gamma)/\text{Br}(\mu^+ \rightarrow e^+e^-e^+)$ and $\text{R}(\mu^- \rightarrow e^- \text{ in nuclei})/\text{Br}(\mu^+ \rightarrow e^+e^-e^+)$ do not depend on the R-parity violating couplings $\lambda_{131}\lambda_{231}$, and only depend on

the SUSY mass spectrum through $m_{\tilde{\nu}_\tau}^2$ and $m_{\tilde{e}_R}^2$:

$$\frac{\text{Br}(\mu^+ \rightarrow e^+ \gamma)}{\text{Br}(\mu^+ \rightarrow e^+ e^- e^+)} = \frac{4 \times 10^{-4} \left(1 - \frac{m_{\tilde{\nu}_\tau}^2}{2m_{\tilde{e}_R}^2}\right)^2}{\beta} = 1 \times 10^{-4}, \quad (4.4)$$

$$\begin{aligned} \frac{\text{R}(\mu^- \rightarrow e^- \text{ in Ti (Al)})}{\text{Br}(\mu^+ \rightarrow e^+ e^- e^+)} &= \frac{2 (1) \times 10^{-5}}{\beta} \left(\frac{5}{6} + \frac{m_{\tilde{\nu}_\tau}^2}{12m_{\tilde{e}_R}^2} + \log \frac{m_e^2}{m_{\tilde{\nu}_\tau}^2} + \delta \right)^2, \\ &= 2 (1) \times 10^{-3}, \end{aligned} \quad (4.5)$$

the second of the equal signs being valid for $m_{\tilde{\nu}_\tau} = m_{\tilde{e}_R} = 100$ GeV. Here $\beta = 1 + (\text{one-loop contr.})/(\text{tree-level contr.})$ in the $\mu^+ \rightarrow e^+ e^- e^+$ process, which is close to unity (for example, $\beta = 0.98$ for $m_{\tilde{\nu}_\tau} = m_{\tilde{e}_R} = 100$ GeV). Since the $\mu^+ \rightarrow e^+ e^- e^+$ process is generated at tree level, its branching ratio is much larger than that of the other LFV processes, as expected. If such a scenario were realized in nature, the $\mu^+ \rightarrow e^+ e^- e^+$ process would dominate over all the other channels, *i.e.*, it is very likely that if nature realizes this particular scenario, $\mu^+ \rightarrow e^+ e^- e^+$ is within experimental reach while $\mu^+ \rightarrow e^+ \gamma$ is orders of magnitude below any foreseeable future experiment.

Another interesting feature of Eqs.(4.4,4.5) is that, because of an ultraviolet log-enhancement of the off-shell photon penguin contribution (A_1^L) [20, 30], the $\mu^- \rightarrow e^-$ conversion rates are significantly larger than the branching ratio of $\mu^+ \rightarrow e^+ \gamma$.

It is important to emphasise that the ratios of branching ratios of the different processes are very different from those in the different neutrino-mass models. For example, in the MSSM with heavy right-handed neutrinos (and R-parity conservation) [7], the following relations are approximately satisfied, because the on-shell photon penguin contribution A_2^R tends to dominate over all others:

$$\frac{\text{Br}(\mu^+ \rightarrow e^+ \gamma)}{\text{Br}(\mu^+ \rightarrow e^+ e^- e^+)} \simeq \frac{3\pi}{\alpha \left(\log \frac{m_\mu^2}{m_e^2} - \frac{11}{4} \right)} = 1.6 \times 10^2, \quad (4.6)$$

$$\frac{\text{R}(\mu^- \rightarrow e^- \text{ in Ti})}{\text{Br}(\mu^+ \rightarrow e^+ e^- e^+)} \simeq \frac{\alpha^3 Z_{eff}^4 |F(q)|^2 m_\mu^5 G_F^2}{4\pi^2 \left(\log \frac{m_\mu^2}{m_e^2} - \frac{11}{4} \right) \Gamma(\mu \text{ capture})} = 0.92 \quad (4.7)$$

Another interesting feature of the case at hand is that in the $\mu^+ \rightarrow e^+ e^- e^+$ process we obtain the following P-odd asymmetries (Eqs. (3.6-3.7)):

$$A_{P_1} \simeq \frac{3(0.12C_4)}{2(0.96C_4)} = 19\%, \quad (4.8)$$

$$A_{P_2} \simeq \frac{-3(0.1C_4)}{2(0.96C_4)} = -15\%, \quad (4.9)$$

$$\frac{A_{P_1}}{A_{P_2}} \simeq -1.3, \quad (4.10)$$

since the tree-level contribution B^L (C_4) is dominant. The key feature here is that the two different P-odd asymmetries have opposite sign; $A_{P_1}/A_{P_2} \simeq -1.3$. More generally, this feature is present whenever the effective vertices $B^{L,R}$ are dominant. In Table 1 we list results of other similar examples.

The situation is clearly different from the MSSM with heavy right-handed neutrinos, where the on-shell photon contributions A_2^R (C_5) are dominant (this case is also listed in Table 1, in order to facilitate comparisons):

$$\begin{aligned} A_{P_1} &\simeq \frac{3(5.6C_5)}{2(87C_5)} = 10\%, \quad A_{P_2} \simeq \frac{3(10C_5)}{2(87C_5)} = 17\%, \\ \frac{A_{P_1}}{A_{P_2}} &\simeq 0.6. \end{aligned} \quad (4.11)$$

Therefore, a measurement of the (sign of the) ratio of P-odd asymmetries in $\mu^+ \rightarrow e^+e^-e^+$ can clearly separate these two models ($B_{L,R} \gg A_i^{L,R}$ versus $A_2^{L,R} \gg B_{L,R}$).

Another useful observable which may be measured in the case one has access to polarised muon decays is A_P (Eq. (3.4)). In RPV models, A_P can have different values (see Table 1), while in other SUSY extensions of the SM, either $\mu^+ \rightarrow e_L^+\gamma$ or $\mu^+ \rightarrow e_R^+\gamma$ is forbidden. Some examples include R-parity conserving SUSY with right-handed neutrinos (see Table 1), $SU(5)$ and $SO(10)$ SUSY grand unified theories, and other MSSM extensions [31, 9].

4.2 All processes induced at one-loop level

Here we consider a different representative case, in which all of $\mu^+ \rightarrow e^+\gamma$, $\mu^+ \rightarrow e^+e^-e^+$, and $\mu^- \rightarrow e^-$ conversion in nuclei are induced at the one-loop level (at the lowest order in RPV couplings) through the photon penguin diagram (Fig. 2). Suppose, as an example, that only the couplings λ_{132} and λ_{232} are nonzero (again we assume that both of them are real, without loss of generality). The effective vertices for the LFV processes are

Table 1: *The ratios of branching ratios $\text{Br}(\mu^+ \rightarrow e^+ \gamma)/\text{Br}(\mu^+ \rightarrow e^+ e^- e^+)$ and $\text{R}(\mu^- \rightarrow e^- \text{ in Ti})/\text{Br}(\mu^+ \rightarrow e^+ e^- e^+)$, P -odd asymmetries A_P for $\mu^+ \rightarrow e^+ \gamma$, A_{P_1} and A_{P_2} for $\mu^+ \rightarrow e^+ e^- e^+$ are shown when the listed pair of Yukawa couplings is dominant. Case (1), (2), (3) refers to the representative classes of models discussed in Secs. 4.1, 4.2, and 4.3, respectively. Here, we assume $m_{\tilde{\nu}, \tilde{l}_R} = 100$ GeV and no mixing in the charged slepton mass matrix, and $m_{\tilde{q}} = 300$ GeV. We also show a typical result obtained for the MSSM with heavy right-handed neutrinos and R -parity conservation [7].*

	$\frac{\text{Br}(\mu \rightarrow e \gamma)}{\text{Br}(\mu \rightarrow 3e)}$	$\frac{\text{R}(\mu \rightarrow e \text{ in Ti})}{\text{Br}(\mu \rightarrow 3e)}$	A_P	A_{P_1}	A_{P_2}	A_{P_1}/A_{P_2}
Case (1)						
$\lambda_{131} \lambda_{231}$	1×10^{-4}	2×10^{-3}	−100%	+19%	−15%	−1.3
$\lambda_{121} \lambda_{122}$	8×10^{-4}	7×10^{-3}	+100%	−19%	+15%	−1.3
$\lambda_{131} \lambda_{132}$	8×10^{-4}	5×10^{-3}	+100%	−19%	+15%	−1.3
Case (2)						
$\lambda_{132} \lambda_{232}$	1.2	18	−100%	−25%	−5%	5.6
$\lambda_{133} \lambda_{233}$	3.7	18	−100%	−25%	−4%	6.2
$\lambda_{231} \lambda_{232}$	3.6	18	+100%	+25%	+4%	6.2
$\lambda'_{122} \lambda'_{222}$	1.4	18	−100%	−25%	−4%	5.7
$\lambda'_{123} \lambda'_{223}$	2.2	18	−100%	−25%	−4%	5.9
Case (3)						
$\lambda'_{111} \lambda'_{211}$	0.4	3×10^2	−100%	−26%	−5%	5.4
$\lambda'_{112} \lambda'_{212}$	0.5	8×10^4	−100%	−26%	−5%	5.4
$\lambda'_{113} \lambda'_{213}$	0.7	1×10^5	−100%	−26%	−5%	5.5
$\lambda'_{121} \lambda'_{221}$	1.1	2×10^5	−100%	−26%	−5%	5.6
MSSM with ν_R	1.6×10^2	0.92	−100%	10%	17%	0.6

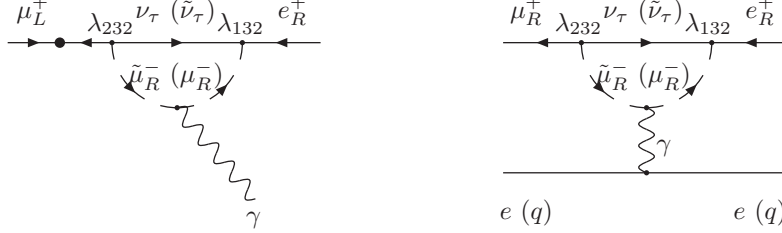


Figure 2: Lowest order Feynman diagrams for lepton flavour violating processes induced by $\lambda_{132}\lambda_{232}$ couplings (see Eq. (2.1)).

$$A_2^R = -\frac{\lambda_{132}\lambda_{232}}{96\pi^2 m_{\tilde{\nu}_\tau}^2} \left(1 - \frac{m_{\tilde{\nu}_\tau}^2}{2m_{\tilde{\mu}_R}^2}\right), \quad (4.12)$$

$$A_1^L = \frac{\lambda_{132}\lambda_{232}}{96\pi^2 m_{\tilde{\nu}_\tau}^2} \left(-\frac{8}{3} - 2\log \frac{m_\mu^2}{m_{\tilde{\nu}_\tau}^2} + \frac{m_{\tilde{\nu}_\tau}^2}{3m_{\tilde{\mu}_R}^2} - \delta(m_\mu^2/q^2)\right). \quad (4.13)$$

Again, we set $q^2 = -m_\mu^2$ for $\mu^- \rightarrow e^-$ conversion, and $q^2 = 0$ for $\mu^+ \rightarrow e^+e^-e^+$.⁵ The ratios of branching ratios $\text{Br}(\mu^+ \rightarrow e^+\gamma)/\text{Br}(\mu^+ \rightarrow e^+e^-e^+)$ and $\text{R}(\mu^- \rightarrow e^- \text{ in nuclei})/\text{Br}(\mu^+ \rightarrow e^+e^-e^+)$ are independent on the choice of $\lambda_{132}\lambda_{232}$:

$$\begin{aligned} \frac{\text{Br}(\mu^+ \rightarrow e^+\gamma)}{\text{Br}(\mu^+ \rightarrow e^+e^-e^+)} &= 3.2 \times 10^3 \frac{\left(1 - \frac{m_{\tilde{\nu}_\tau}^2}{2m_{\tilde{\mu}_R}^2}\right)^2}{\left(-\frac{8}{3} - 2\log \frac{m_\mu^2}{m_{\tilde{\nu}_\tau}^2} + \frac{m_{\tilde{\nu}_\tau}^2}{3m_{\tilde{\mu}_R}^2}\right)^2 \gamma}, \\ &= 1.2, \end{aligned} \quad (4.14)$$

$$\begin{aligned} \frac{\text{R}(\mu^- \rightarrow e^- \text{ in Ti (Al)})}{\text{Br}(\mu^+ \rightarrow e^+e^-e^+)} &= 19.5 \text{ (11.5)} \frac{\left(\frac{5}{3} + \frac{m_{\tilde{\nu}_\tau}^2}{6m_{\tilde{\mu}_R}^2} + 2\log \frac{m_\mu^2}{m_{\tilde{\nu}_\tau}^2} + \delta\right)^2}{\left(-\frac{8}{3} - 2\log \frac{m_\mu^2}{m_{\tilde{\nu}_\tau}^2} + \frac{m_{\tilde{\nu}_\tau}^2}{3m_{\tilde{\mu}_R}^2}\right)^2 \gamma}, \\ &= 18 \text{ (11)}, \end{aligned} \quad (4.15)$$

⁵Since the log-term is much larger than the δ term for $0 < q^2 < m_\mu^2$ in Eq. (4.13), the result does not depend significantly on the choice of q in the $\mu^+ \rightarrow e^+e^-e^+$ process.

where the second of the equal signs holds for $m_{\tilde{\nu}_\tau} = m_{\tilde{\mu}_R} = 100$ GeV. Here γ is a function of the SUSY mass spectrum, but it is of order unity.

$$\gamma = 1 + \frac{\frac{8}{3}|A_2^R|^2 \left(\log \frac{m_\mu^2}{m_e^2} - \frac{11}{4} \right) - 4\text{Re}(A_1^L A_2^R)}{|A_1^L|^2}. \quad (4.16)$$

As an example, $\gamma = 1.09$ for $m_{\tilde{\nu}_\tau} = m_{\tilde{\mu}_R} = 100$ GeV.

Because of the ultraviolet log-enhancement of the off-shell photon penguin diagram (A_1^L) in Eq.(4.13), the event rates for the $\mu^+ \rightarrow e^+e^-e^+$ and $\mu^- \rightarrow e^-e^+e^-$ conversion in nuclei can be as large as the branching ratio for the $\mu^+ \rightarrow e^+\gamma$ process, even though they are higher order processes in QED.⁶ Fig. 3 depicts the dependence on the slepton masses of these ratios of branching ratios. In the case of $\mu^+ \rightarrow e^+\gamma$, a cancellation between the two different diagrams (sneutrino and smuon loops) can occur, such that its branching ratio can be much smaller than that of the other processes. On the other hand, the numerical value of the ratio $\text{R}(\mu^- \rightarrow e^- \text{ in nuclei})/\text{Br}(\mu^+ \rightarrow e^+e^-e^+)$ is stable in a large region of the parameter space. All the LFV processes are equally relevant in this model. Again, we stress that these ratios of the branching ratios are very different in more “traditional” cases, such as in the MSSM with heavy right-handed neutrinos (see Eqs.(4.6,4.7)).

Since the off-shell photon diagram A_1^L is dominant in the $\mu^+ \rightarrow e^+e^-e^+$ process, C_2 ($= C_4$) in Eqs.(3.9,3.10) is much larger than the other C_i ($i \neq 2, 4$). In this case, the P-odd asymmetries behave as follows:

$$A_{P_1} \simeq \frac{3(-0.61C_2 + 0.12C_4)}{2(1.8C_2 + 0.96C_4)} = -26\% \quad (4.17)$$

$$A_{P_2} \simeq \frac{3(-0.1C_4)}{2(1.8C_2 + 0.96C_4)} = -5\% \quad (4.18)$$

$$\frac{A_{P_2}}{A_{P_1}} \simeq 0.19. \quad (4.19)$$

These relations (Eqs.(4.14,4.15,4.19)) are a typical feature of models in which the off-shell photon diagram is the dominant contribution to the $\mu^+ \rightarrow e^-e^+e^-$ process. The results of other similar examples are also listed in Table 1.

⁶In the case of $\mu^+ \rightarrow e^+e^-e^+$, there is also an infrared log-enhancement to the branching ratio, as can be seen in Eq. (3.19).

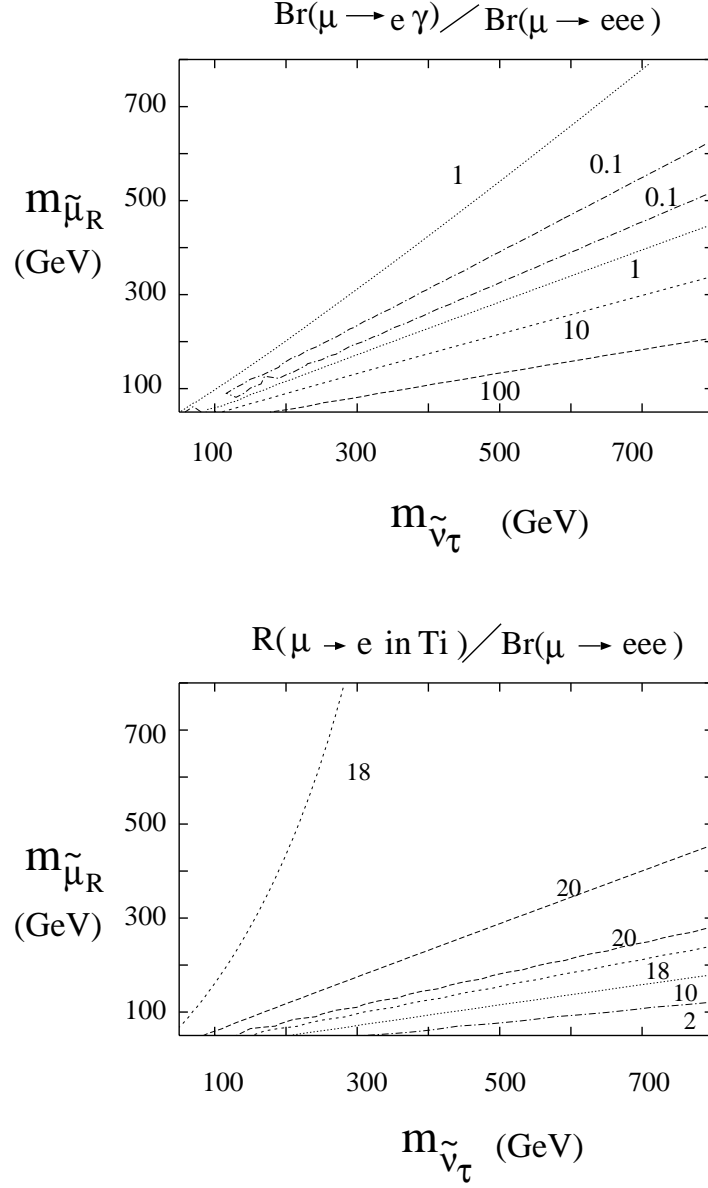


Figure 3: Contours of constant $\text{Br}(\mu^+ \rightarrow e^+ \gamma) / \text{Br}(\mu^+ \rightarrow e^+ e^- e^+)$ (top), and $R(\mu^- \rightarrow e^- \text{ in Ti}) / \text{Br}(\mu^+ \rightarrow e^+ e^- e^+)$ (bottom) in the $(m_{\tilde{\mu}_R} \times m_{\tilde{\nu}_\tau})$ plane, assuming that only the product of $LL\bar{E}$ couplings $\lambda_{132}\lambda_{232}$ is non-zero (see Eq. (2.1)).

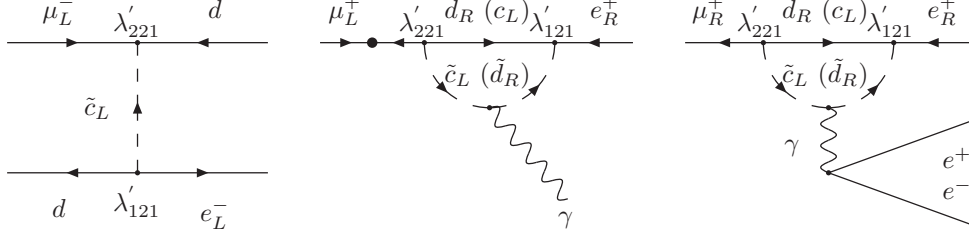


Figure 4: Lowest order Feynman diagrams of lepton flavour violating processes induced by $f'_{121}f'_{221}$ couplings (see Eq. (2.1)).

4.3 $\mu^- \rightarrow e^-$ conversion in nuclei induced at tree-level

Here, we consider the possibility that $\mu^- \rightarrow e^-$ conversion in nuclei is induced at tree-level. This can arise through some of the $LQ\bar{D}$ terms (λ'_{ijk}). As an example, we consider a model in which only λ'_{121} and λ'_{221} are non-zero, so $\mu^- \rightarrow e^-$ conversion is generated at tree-level while $\mu^+ \rightarrow e^+\gamma$ and $\mu^+ \rightarrow e^+e^-e^+$ are generated at one-loop level (Fig. 4).

The LFV vertices are

$$D^d = -\frac{f'_{121}\lambda'_{221}}{2m_{\tilde{c}_L}^2}, \quad A_2^R = -\frac{f'_{121}\lambda'_{221}}{64\pi^2 m_{\tilde{d}_R}^2}, \quad (4.20)$$

$$A_1^L = \frac{f'_{121}\lambda'_{221}}{96\pi^2 m_{\tilde{d}_R}^2} \left\{ -5 - 4 \log \frac{m_c^2}{m_{\tilde{d}_R}^2} - \frac{2}{3} \delta(m_c^2/q^2) + \frac{m_{\tilde{d}_R}^2}{m_{\tilde{c}_L}^2} \left(-2 - 2 \log \frac{m_d^2}{m_{\tilde{c}_L}^2} - \frac{1}{3} \delta(m_d^2/q^2) \right) \right\}. \quad (4.21)$$

As before, we set $q^2 = -m_\mu^2$ for $\mu^- \rightarrow e^-$ conversion, and $q^2 = 0$ for $\mu^+ \rightarrow e^+e^-e^+$. The ratios of branching ratios are

$$\frac{\text{Br}(\mu^+ \rightarrow e^+\gamma)}{\text{Br}(\mu^+ \rightarrow e^+e^-e^+)} = 1.1, \quad (4.22)$$

$$\frac{\text{R}(\mu^- \rightarrow e^- \text{ in Ti (Al)})}{\text{Br}(\mu^+ \rightarrow e^+e^-e^+)} = 2 (1) \times 10^5. \quad (4.23)$$

Here we assume $m_{\tilde{d}_R} = m_{\tilde{c}_L} = 300$ GeV. Since $\mu^- \rightarrow e^-$ conversion is

induced at the tree-level, its event rate is much larger than that of other processes, as expected.

In $\mu^+ \rightarrow e^+e^-e^+$, the off-shell photon penguin vertex (A_1^L) dominates over the other contributions because of the ultraviolet log-enhancement. Therefore, the ratio of branching ratios $\text{Br}(\mu^+ \rightarrow e^+\gamma)/\text{Br}(\mu^+ \rightarrow e^+e^-e^+)$ and the P-odd asymmetries A_{P_1} and A_{P_2} (which are presented in Table 1) are very similar to those we obtained in the previous subsection. The order one numerical differences come from the different sfermion masses used in both cases and the fact that there are quarks and not leptons running around the loops. Results for other similar examples are also listed in Table 1.

In the case of $\mu^+ \rightarrow e^+e^-e^+$, the fact that we choose a fixed value of $q^2(=0)$ instead of integrating over all possible q^2 values leads to some uncertainty. These, however, are not important as far as our intentions here are concerned. We note that the numbers presented in Table 1 for ratios of branching ratios when there are first generation quarks running around the loops are uncertain by some tens of percent.

4.4 Large T-odd Asymmetry in $\mu^+ \rightarrow e^+e^-e^+$

It is important to understand if any interesting effect can be obtained if more than a single pair of RPV couplings is present. Here we consider the possibility that $\mu^+ \rightarrow e^+e^-e^+$ is generated at the tree-level, but that the loop-level contributions of on-shell (and off-shell) photons is comparable. This can be accomplished by having, for example, nonzero $\lambda_{131}\lambda_{231}$ and $\lambda_{133}\lambda_{233} \gg \lambda_{131}\lambda_{231}$.

In this case, all of B^L , A_1^L , and A_2^R can be comparable, and there is the possibility that the T-odd asymmetry in $\mu^+ \rightarrow e^+e^-e^+$ decay (Eq.(3.8)) is large. We proceed to discuss this in more detail.

We will consider the most general case in which all effective couplings B^L , A_1^L , and A_2^R are independent (as may be effectively the case if many RPV couplings are relevant). In this case, the T-odd asymmetry (Eq.(3.8)) can be written as

$$\begin{aligned} A_T &= \frac{3(a_{11}C_{11} - a_{12}C_{12})}{2(a_2C_2 + a_4C_4 + a_5C_5 + a_7C_7 + a_9C_9)}, \\ &= \frac{3a_{11}x \sin(\theta_2 - \theta_1) - 3a_{12}\{y \sin \theta_2 + x \sin(\theta_2 - \theta_1)\}}{X}, \end{aligned} \quad (4.24)$$

where

$$X = 4a_2x^2 + 4a_4(x^2 + y^2 + 2xy \cos \theta_1) + a_5 - 2a_7x \cos(\theta_2 - \theta_1) - 2a_9\{y \cos \theta_2 + x \cos(\theta_2 - \theta_1)\}.$$

Here $(a_2, a_4, a_5, a_7, a_9, a_{11}, a_{12}) = (1.8, 0.96, 88, 14, 7.5, 2.0, 1, 6)$, $x = |A_1^L/A_2^R|$, $y = |B^L/4\pi\alpha A_2^R|$, and θ_1 (θ_2) is the relative phase between B^L and A_1^L (A_2^R). Even when x, y, θ_1 and θ_2 are treated as independent parameters, this T-odd asymmetry has a maximum value,

$$A_T|_{\max} = 24\%, \quad (4.25)$$

when

$$\begin{aligned} x &= \left| \frac{A_1^L}{A_2^R} \right| = 2.56, \\ y &= \left| \frac{B^L}{4\pi\alpha A_2^R} \right| = 4.23, \\ \theta_1 &= -2.28, \\ \theta_2 &= -1.56. \end{aligned} \quad (4.26)$$

This upper limit is quite general, and applies to any extension of the SM. It can be obtained directly from the most general effective Lagrangian which parametrises $\mu^+ \rightarrow e^+e^-e^+$ [32].

Fig. 5 depicts the value of the T-odd asymmetry and the ratio of branching ratios of $\mu^+ \rightarrow e^+\gamma$ and $\mu^+ \rightarrow e^+e^-e^+$, when we fix $\theta_1 = -2.28$, $\theta_2 = -1.56$ (same as at the maximum point). As can be seen from Fig. 5, these two observables are strongly correlated. In the region where the T-odd asymmetry is relatively large, the branching ratio for $\mu^+ \rightarrow e^+\gamma$ tends to be much bigger than the one for $\mu^+ \rightarrow e^+e^-e^+$, since an on-shell photon coupling A_2^R comparable to A_1^R and B^L is required in order to obtain a large T-odd asymmetry. In this case, the branching ratio of $\mu^+ \rightarrow e^+e^-e^+$ is dominated by the A_2^R coefficient due to the relatively large collinear infrared logarithm (see Eq. (3.19)) and we obtain a ratio of branching ratios similar to the one obtained for the MSSM with heavy right-handed neutrinos (Eq. (4.6)).

In a generic RPV model, the T-odd asymmetry is unlikely to be close to its maximum value (Eq.(4.25)) because the branching ratio for $\mu^+ \rightarrow e^+e^-e^+$ is expected to be comparable to (an in some cases even much larger than) the one for $\mu^+ \rightarrow e^+\gamma$, as we argued in the previous subsections. It is,

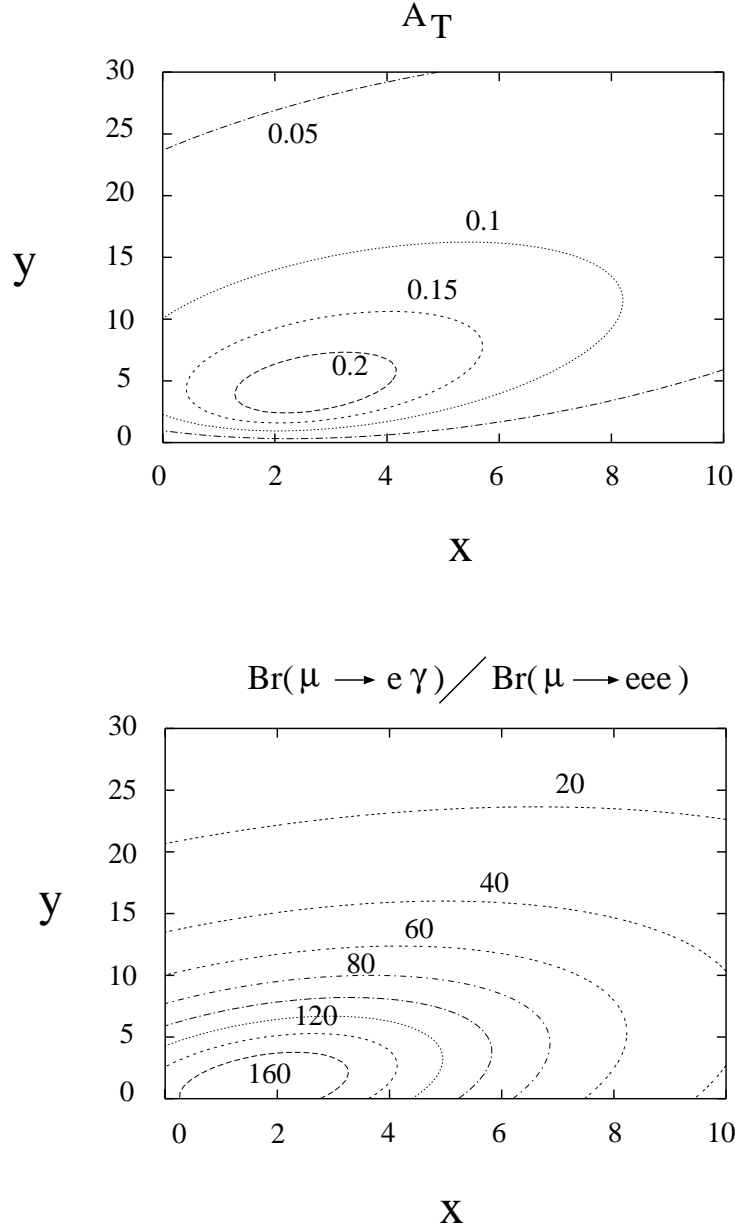


Figure 5: Constant contours of the T -odd asymmetry (top) and the ratio of branching ratios $\text{Br}(\mu^+ \rightarrow e^+ \gamma) / \text{Br}(\mu^+ \rightarrow e^+ e^- e^+)$ (bottom) in the $(x \times y)$ plane. $x = |\frac{A_1^L}{A_2^R}|$ and $y = |\frac{B^L}{4\pi\alpha A_2^R}|$. The relative phases between B^L, A_2^R and A_1^L, A_2^R are fixed at $(\theta_1, \theta_2) = (-2.28, -1.56)$. See text for details.

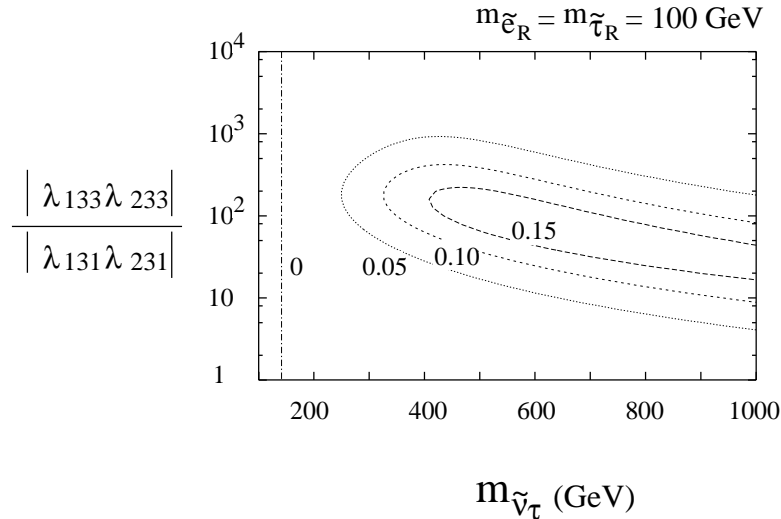


Figure 6: *Constant contours of the T-odd asymmetry and the in the $(m_{\tilde{\nu}_\tau} \times |\lambda_{133}\lambda_{233}/\lambda_{131}\lambda_{231}|)$ plane, assuming that all other RPV couplings vanishes and that the relative phase between the two pairs of copings is $\pi/2$.*

however, possible to tune the various parameters in order to achieve large effects. In other SUSY extensions of the SM, large T-odd asymmetries can also be obtained in particular regions of parameter space. For example, the authors of [27] discuss LFV in the case of SUSY grand unified theories, and find T-odd asymmetries larger than 15% in some $SU(5)$ models.

As an example, consider a situation where $\lambda_{131}\lambda_{213}^* = 10^{-6}$ and $\lambda_{133}\lambda_{233}^* = 1.6 \times 10^{-4} e^{i\frac{\pi}{2}}$, while all other RPV couplings are zero, leading to $A_T = 17\%$ for $m_{\tilde{\nu}_\tau} = 500$ GeV and $m_{\tilde{e}_R} = m_{\tilde{\tau}_R} = 100$ GeV. Here $\text{Br}(\mu^+ \rightarrow e^+ \gamma) = 5 \times 10^{-12}$ and $\text{Br}(\mu^+ \rightarrow e^+ e^- e^+) = 3 \times 10^{-14}$. Note that, in order to obtain large A_T values, one is required to impose a mild hierarchy in the ratios of scalar masses (order 10^1) and a more severe, finely-tuned hierarchy in the ratio of couplings (order 10^2), as is illustrated in Fig. 6.

5 Conclusions

We discussed lepton flavour violation (LFV) in rare muon processes ($\mu^+ \rightarrow e^+ \gamma$, $\mu^+ \rightarrow e^+ e^- e^+$, $\mu^- \rightarrow e^-$ conversion in nuclei) in SUSY models with

trilinear R-parity violation (RPV). Such models are interesting in the sense that they can accommodate neutrino masses without requiring the introduction of extra fields to the MSSM. Natural explanations for the smallness of the RPV couplings have been studied [16], and are not discussed here.

It is well known that LFV in the charged lepton sector is a very sensitive probe for models with RPV, and that some of the most stringent constraints on RPV couplings come from LFV processes. Here, instead of concentrating on how RPV couplings are constrained by LFV, we study the expectations for LFV observables in the case nature realizes SUSY with small RPV, and discuss a number of different observables which may play a decisive role in distinguishing RPV models among themselves and from other SUSY models.

Along these lines, we considered a number of representative cases for different RPV models in order to understand a number of features related to LFV. An important observation is that, in generic RPV models, all of the LFV processes considered are of the same order (*i.e.* the ratio of branching ratios is of order one), or $\mu^+ \rightarrow e^+ \gamma$ is very suppressed with respect to either $\mu^+ \rightarrow e^+ e^- e^+$ and/or $\mu^- \rightarrow e^-$ conversion in nuclei, as is summarised in Table 1. This behaviour is to be compared with R-conserving SUSY models with heavy right-handed neutrinos, where the branching ratio of $\mu^+ \rightarrow e^+ \gamma$ is always much larger than the branching ratio for $\mu^+ \rightarrow e^+ e^- e^+$ and (in general) the rate for $\mu^- \rightarrow e^-$ conversion in nuclei.

We also argue that the P-odd and T-odd asymmetries which can be measured in the case of polarised $\mu^+ \rightarrow e^+ e^- e^+$ decays give an extra handle when it comes to distinguishing different models. In particular, we discussed whether a large T-odd asymmetry can be generated in the case of RPV SUSY.

In summary, if there is indeed low-energy SUSY with small but non-negligible RPV couplings, it is likely that these not only contribute to Majorana neutrino masses but also will be probed by LFV in the charged lepton sector. If this is the case, naively higher order QED processes, such as $\mu^+ \rightarrow e^+ e^- e^+$ or $\mu^- \rightarrow e^-$ conversion in nuclei are at least as relevant as the more canonical $\mu^+ \rightarrow e^+ \gamma$ decay.

Independently of what the new physics beyond the SM is, it should be kept in mind that improving the current experimental sensitivity of *all* LFV processes is important. We hope to discuss this important issue in a future publication [32]. We conclude by stressing that there are proposals for improving the sensitivity to $\mu^+ \rightarrow e^+ \gamma$ down to branchings ratios of 10^{-14} [33] and the sensitivity to $\mu^- \rightarrow e^-$ conversion in nuclei down to rates of 10^{-16}

[34] (see Appendix B); however, in the case of the $\mu^+ \rightarrow e^+e^-e^+$, there are no proposals for improving the current best bound, which is already twelve years old! In view of the results discussed here, we believe that experiments which are sensitive to smaller branching ratios for $\mu^+ \rightarrow e^+e^-e^+$ (at least as sensitive as the future $\mu^+ \rightarrow e^+\gamma$ experiments) are of the utmost importance.

Acknowledgements

We are indebted to Gian Giudice for many enlightening discussions and also thank him for carefully reading the manuscript and providing useful comments. We acknowledge the Stopped Muon Working Group for a Future Muon Storage Ring at CERN for interesting discussions. We also thank T. Yanagida for useful comments.

A LFV effective vertices in trilinear RPV

In this Appendix, we present explicit expressions for the LFV effective vertices $A_{1,2}^{L,R}$, $B^{L,R}$, and $D^{u,d}$ in the trilinear RPV models considered in the body of this paper.

A.1 Photon penguin vertices

The photon penguin vertices are defined in Eq.(3.1). The effective couplings $A_i^{L(R)}$ ($i = 1, 2$) are given by

$$A_i^{R(L)} = A_i^{R(L)(e)} + A_i^{R(L)(\nu)} + A_i^{R(L)(u)} + A_i^{R(L)(d)}, \quad (\text{A.1})$$

where $A_i^{R(L)(e,\nu)}$ are induced by R-parity violating $LL\bar{E}$ couplings through a lepton–sneutrino loop and a neutrino–slepton loop, respectively. $A_i^{R(L)(u,d)}$ are generated by $LQ\bar{D}$ couplings through an up-type quark–down-type squark loop and a down-type quark–up-type squark loop, respectively. The explicit expressions for the on-shell photon vertices A_2 are as follows:

$$A_2^{R(e)} = -\frac{\lambda_{13j}\lambda_{23j}^*}{16\pi^2 m_{\tilde{\nu}3}^2} J_\sigma^{(1)} \left(\frac{m_{e_j}^2}{m_{\tilde{\nu}3}^2}, \frac{q^2}{m_{\tilde{\nu}3}^2}, \frac{m_\mu^2}{m_{\tilde{\nu}3}^2} \right), \quad (\text{A.2})$$

$$A_2^{R(\nu)} = \frac{\lambda_{13j}\lambda_{23j}^*}{16\pi^2 m_{\tilde{e}_{Rj}}^2} J_\sigma^{(2)} \left(\frac{m_{\nu 3}^2}{m_{\tilde{e}_{Rj}}^2}, \frac{q^2}{m_{\tilde{e}_{Rj}}^2}, \frac{m_\mu^2}{m_{\tilde{e}_{Rj}}^2} \right), \quad (\text{A.3})$$

$$A_2^{L(e)} = -\frac{\lambda_{ij1}^* \lambda_{ij2}}{16\pi^2 m_{\tilde{\nu}i}^2} J_\sigma^{(1)} \left(\frac{m_{e_j}^2}{m_{\tilde{\nu}i}^2}, \frac{q^2}{m_{\tilde{\nu}i}^2}, \frac{m_\mu^2}{m_{\tilde{\nu}i}^2} \right), \quad (\text{A.4})$$

$$A_2^{L(\nu)} = \frac{\lambda_{ij1}^* \lambda_{ij2}}{16\pi^2 m_{\tilde{e}Lj}^2} J_\sigma^{(2)} \left(\frac{m_{\nu_i}^2}{m_{\tilde{e}Lj}^2}, \frac{q^2}{m_{\tilde{e}Lj}^2}, \frac{m_\mu^2}{m_{\tilde{e}Lj}^2} \right), \quad (\text{A.5})$$

$$A_2^{R(u)} = -\frac{\lambda'_{1ij} \lambda_{2ij}^*}{16\pi^2 m_{\tilde{d}Rj}^2} \left\{ 2J_\sigma^{(1)} \left(\frac{m_{u_i}^2}{m_{\tilde{d}Rj}^2}, \frac{q^2}{m_{\tilde{d}Rj}^2}, \frac{m_\mu^2}{m_{\tilde{d}Rj}^2} \right) - J_\sigma^{(2)} \left(\frac{m_{u_i}^2}{m_{\tilde{d}Rj}^2}, \frac{q^2}{m_{\tilde{d}Rj}^2}, \frac{m_\mu^2}{m_{\tilde{d}Rj}^2} \right) \right\}, \quad (\text{A.6})$$

$$A_2^{R(d)} = -\frac{\lambda'_{1ij} \lambda_{2ij}^*}{16\pi^2 m_{\tilde{u}Li}^2} \left\{ J_\sigma^{(1)} \left(\frac{m_{d_j}^2}{m_{\tilde{u}Li}^2}, \frac{q^2}{m_{\tilde{u}Li}^2}, \frac{m_\mu^2}{m_{\tilde{u}Li}^2} \right) - 2J_\sigma^{(2)} \left(\frac{m_{d_j}^2}{m_{\tilde{u}Li}^2}, \frac{q^2}{m_{\tilde{u}Li}^2}, \frac{m_\mu^2}{m_{\tilde{u}Li}^2} \right) \right\}, \quad (\text{A.7})$$

$$A_2^{L(u)} = A_2^{L(d)} = 0. \quad (\text{A.8})$$

Here the functions $J_\sigma^{(1,2)}$ are defined by

$$J_\sigma^{(1)}(a, b, c) = \int_0^1 dy \int_0^{1-y} dx \frac{x(1-x-y)}{x\{1-c(1-x-y)\} + a(1-x) - by(1-x-y)} \quad (\text{A.9})$$

$$J_\sigma^{(2)}(a, b, c) = \int_0^1 dy \int_0^{1-y} dx \frac{y(1-x-y)}{x+y-cy(1-x-y) + a(1-x-y) - bxy}. \quad (\text{A.10})$$

When $b, c \ll 1$, these functions can be approximated by

$$J_\sigma^{(1)}(a, b, c) = \frac{2 + 3a - 6a^2 + a^3 + 6a \log a}{12(1-a)^4}, \quad (\text{A.11})$$

$$J_\sigma^{(2)}(a, b, c) = \frac{1 - 6a + 3a^2 + 2a^3 - 6a^2 \log a}{12(1-a)^4}. \quad (\text{A.12})$$

The off-shell photon vertices A_1 are expressed as follows:

$$A_1^{L(e)} = \frac{\lambda_{13j} \lambda_{23j}^*}{16\pi^2 m_{\tilde{\nu}3}^2} J_q^{(1)} \left(\frac{m_{e_j}^2}{m_{\tilde{\nu}3}^2}, \frac{q^2}{m_{\tilde{\nu}3}^2}, \frac{m_\mu^2}{m_{\tilde{\nu}3}^2} \right), \quad (\text{A.13})$$

$$A_1^{L(\nu)} = -\frac{\lambda_{13j} \lambda_{23j}^*}{16\pi^2 m_{\tilde{e}Rj}^2} J_q^{(2)} \left(\frac{m_{\nu_3}^2}{m_{\tilde{e}Rj}^2}, \frac{q^2}{m_{\tilde{e}Rj}^2}, \frac{m_\mu^2}{m_{\tilde{e}Rj}^2} \right), \quad (\text{A.14})$$

$$A_1^{R(e)} = \frac{\lambda_{ij1}^* \lambda_{ij2}}{16\pi^2 m_{\tilde{\nu}i}^2} J_q^{(1)} \left(\frac{m_{e_j}^2}{m_{\tilde{\nu}i}^2}, \frac{q^2}{m_{\tilde{\nu}i}^2}, \frac{m_\mu^2}{m_{\tilde{\nu}i}^2} \right), \quad (\text{A.15})$$

$$A_1^{R(\nu)} = -\frac{\lambda_{ij1}^* \lambda_{ij2}}{16\pi^2 m_{\tilde{e}Lj}^2} J_q^{(2)} \left(\frac{m_{\nu i}^2}{m_{\tilde{e}Lj}^2}, \frac{q^2}{m_{\tilde{e}Lj}^2}, \frac{m_\mu^2}{m_{\tilde{\nu}i}^2} \right), \quad (\text{A.16})$$

$$A_1^{L(u)} = \frac{\lambda'_{1ij} \lambda_{2ij}^*}{16\pi^2 m_{\tilde{d}Rj}^2} \left\{ 2J_q^{(1)} \left(\frac{m_{u_i}^2}{m_{\tilde{d}Rj}^2}, \frac{q^2}{m_{\tilde{d}Rj}^2}, \frac{m_\mu^2}{m_{\tilde{d}Rj}^2} \right) - J_q^{(2)} \left(\frac{m_{u_i}^2}{m_{\tilde{d}Rj}^2}, \frac{q^2}{m_{\tilde{d}Rj}^2}, \frac{m_\mu^2}{m_{\tilde{d}Rj}^2} \right) \right\}, \quad (\text{A.17})$$

$$A_1^{(d)} = \frac{\lambda'_{1ij} \lambda_{2ij}^*}{16\pi^2 m_{\tilde{u}Li}^2} \left\{ J_q^{(1)} \left(\frac{m_{d_j}^2}{m_{\tilde{u}Li}^2}, \frac{q^2}{m_{\tilde{u}Li}^2}, \frac{m_\mu^2}{m_{\tilde{u}Li}^2} \right) - 2J_q^{(2)} \left(\frac{m_{d_j}^2}{m_{\tilde{u}Li}^2}, \frac{q^2}{m_{\tilde{u}Li}^2}, \frac{m_\mu^2}{m_{\tilde{u}Li}^2} \right) \right\}, \quad (\text{A.18})$$

where the functions $J_q^{(1,2)}$ are defined by

$$J_q^{(1)}(a, b, c) = \int_0^1 dy \int_0^{1-y} dx \frac{(x+2y)(1-x-y)}{x\{1-c(1-x-y)\} + a(1-x) - by(1-x-y)} \quad (\text{A.19})$$

$$J_q^{(2)}(a, b, c) = \int_0^1 dy \int_0^{1-y} dx \frac{y(x-y)}{x+y-cy(1-x-y) + a(1-x-y) - bxy}. \quad (\text{A.20})$$

When $a, b, c \ll 1$, these functions are well approximated by

$$J_q^{(1)}(a, b, c) = -\frac{1}{3} \left(\frac{4}{3} + \log a + \delta(a/b) \right), \quad (\text{A.21})$$

$$J_q^{(2)}(a, b, c) = -\frac{1}{18}, \quad (\text{A.22})$$

where

$$\delta(d) = \begin{cases} -\frac{5}{3} - 4d + 2(1+2d)\sqrt{1-4d} \tanh^{-1} \frac{1}{\sqrt{1-4d}}, & \text{for } d < \frac{1}{4} \\ -\frac{5}{3} - 4d + 2(1+2d)\sqrt{4d-1} \tan^{-1} \frac{1}{\sqrt{4d-1}}, & \text{for } d > \frac{1}{4}. \end{cases} \quad (\text{A.23})$$

When $a \gg b, c$ and $b, c \ll 1$,

$$J_q^{(1)}(a, b, c) = \frac{-16 + 45a - 36a^2 + 7a^3 - (12 - 18a) \log a}{36(1-a)^4}, \quad (\text{A.24})$$

$$J_q^{(2)}(a, b, c) = \frac{-2 + 9a - 18a^2 + 11a^3 - 6a^3 \log a}{36(1-a)^4}. \quad (\text{A.25})$$

A.2 Tree-level vertices in the $\mu^+ \rightarrow e^+ e^- e^+$ process

The tree-level vertices $B^{R(L)}$ in the $\mu^+ \rightarrow e^+ e^- e^+$ process are defined in Eq.(3.5). Their explicit expressions are given by

$$B^L = -\frac{\lambda_{i11} \lambda_{i21}^*}{2m_{\tilde{\nu}_i}^2}, \quad (\text{A.26})$$

$$B^R = -\frac{\lambda_{i11}^* \lambda_{i12}}{2m_{\tilde{\nu}_i}^2}. \quad (\text{A.27})$$

A.3 Tree-level vertices in the $\mu^- \rightarrow e^-$ conversion process

The tree-level vertices for $\mu^- \rightarrow e^-$ conversion were defined in Eq.(3.20). Their explicit forms are

$$D^u = \frac{\lambda_{11i}^* \lambda_{21i}'}{2m_{\tilde{d}_{Ri}}^2}, \quad (\text{A.28})$$

$$D^d = -\frac{\lambda_{1j1}^* \lambda_{2j1}'}{2m_{\tilde{u}_{Lj}}^2}. \quad (\text{A.29})$$

B Constraints on R-parity-violating Couplings from LFV Processes and Neutrino Masses

The experimental limits on LFV processes set tight bounds on specific combinations of R-parity violating couplings. The most stringent experimental limit on the branching ratio of $\mu^+ \rightarrow e^+ e^- e^+$ is given by the SINDRUM experiment at PSI [35]:⁷

$$\text{Br}(\mu^+ \rightarrow e^+ e^- e^+)|_{\text{exp.}} < 1.0 \times 10^{-12}. \quad (\text{B.30})$$

⁷In order to reach the current bounds, rare muon decay experiments need to stop the muons before they decay. For this reason, they are constrained to analyse μ^+ decays, since the μ^- is readily captured by the material present in order to stop the muons and there are virtually no free μ^- decays. For the same reason, one can only measure the $\mu \rightarrow e$ conversion rate in nuclei for the μ^- .

The present experimental limit on the branching ratio of $\mu^+ \rightarrow e^+ \gamma$ process is set by the MEGA collaboration at LANL [36]:

$$\text{Br}(\mu^+ \rightarrow e^+ \gamma)|_{\text{exp.}} < 1.2 \times 10^{-11}. \quad (\text{B.31})$$

This limit will be significantly improved (or, perhaps, LFV will be found!) in the near future by a new experiment at PSI [33], which claims to be able to observe $\mu^+ \rightarrow e^+ \gamma$ events if $\text{Br}(\mu^+ \rightarrow e^+ \gamma) > 10^{-14}$. The present experimental bound on the conversion rate of $\mu^- \rightarrow e^-$ in $^{48}_{22}\text{Ti}$ was determined by the SINDRUM 2 collaboration at PSI [37]:

$$\text{R}(\mu^- \rightarrow e^- \text{ in } ^{48}_{22}\text{Ti})|_{\text{exp.}} < 6.1 \times 10^{-13}. \quad (\text{B.32})$$

The future proposed (almost approved) experiment MECO [34] claims that it will be able to see $\mu^- \rightarrow e^-$ conversion in aluminium if $\text{R}(\mu^- \rightarrow e^- \text{ in } ^{27}_{13}\text{Al}) > 10^{-16}$. (More futuristic proposals claim sensitivity to values of the rate of $\mu^- \rightarrow e^-$ conversion in nuclei as low as 10^{-18} [38]!)

Tables 2, 3 contain current and near future bounds on the absolute values of some pairs of RPV couplings, assuming that all other pairs of couplings vanish.

In models with trilinear RPV, neutrino masses are generated at one-loop via squark (slepton) exchange for $LQ\bar{D}$ ($LL\bar{E}$) operators. Under the assumption that the left-right sfermion soft mass-squared mixing terms are diagonal in the physical basis and proportional to the associated fermion mass ($m_{\tilde{f}LR}^2 \propto m_f m_{\tilde{f}}$), the formula for the neutrino masses can be simplified to [15]

$$m_{\nu_{ii'}} \simeq \frac{n_c \lambda_{ijk} \lambda_{ikj}}{16\pi^2} m_{f_j} m_{f_k} \left[\frac{f(m_{f_j}^2/m_{\tilde{f}_k}^2)}{m_{\tilde{f}_k}} + \frac{f(m_{f_k}^2/m_{\tilde{f}_j}^2)}{m_{\tilde{f}_j}} \right] \quad (\text{B.33})$$

$$f(x) = (x \ln x - x + 1)/(x - 1)^2$$

Here, m_{f_i} is the fermion mass of the i th generation inside the loop, $m_{\tilde{f}_i}$ is the average of the \tilde{f}_{Li} and \tilde{f}_{Ri} squark masses, and n_c is a colour factor (3 for $LQ\bar{D}$ operators and 1 for $LL\bar{E}$ operators). This expression implies that the heavier the fermions in the loop, the stricter the bounds [15]. For example, demanding $m_{e\mu} < 1$ eV for sparticle masses of 300 GeV, $m_b = 4.4$ GeV and $m_s = 170$ MeV, leads to $\lambda'_{133} \lambda'_{233} \leq 4 \cdot 10^{-7}$. For $\lambda'_{122} \lambda'_{222}$ the bound drops to $2.3 \cdot 10^{-4}$ [15], while for “Super-Kamiokande-friendly” solutions with

Table 2: Current (future) constraints on the R -parity violating couplings $LL\bar{E}$ (see Eq. (2.1)) from LFV processes, assuming that only the listed pair of coupling is nonzero. The current (future) upper limits on the branching ratios are: $\text{Br}(\mu^+ \rightarrow e^+ \gamma) < 1.2 \times 10^{-11}$ (10^{-14}), $\text{Br}(\mu^+ \rightarrow e^+ e^- e^+) < 1.0 \times 10^{-12}$, and $\text{R}(\mu^- \rightarrow e^- \text{ in Ti}) < 6.1 \times 10^{-13}$ ($\text{R}(\mu^- \rightarrow e^- \text{ in Al}) < 10^{-16}$). Here we assume all the sneutrino masses degenerate with right-handed slepton masses, $m_{\tilde{\nu}, \tilde{l}_R} = 100 \text{ GeV}$, and we neglect left-right mixing in the charged slepton mass matrix. The notation (tree) indicates that the $\mu^+ \rightarrow e^+ e^- e^+$ process is generated at the tree-level.

	$\mu \rightarrow e \gamma$	$\mu \rightarrow eee$	$\mu \rightarrow e \text{ in nuclei}$
$ \lambda_{131} \lambda_{231} $	2.3×10^{-4} [18] (7×10^{-6})	$6.7 \times 10^{-7}(\text{tree})$ [17]	1.1×10^{-5} [20] (2×10^{-7})
$ \lambda_{132} \lambda_{232} $	2.3×10^{-4} [18] (7×10^{-6})	7.1×10^{-5}	1.3×10^{-5} [20] (2×10^{-7})
$ \lambda_{133} \lambda_{233} $	2.3×10^{-4} [18] (7×10^{-6})	1.2×10^{-4}	2.3×10^{-5} [20] (4×10^{-7})
$ \lambda_{121} \lambda_{122} $	8.2×10^{-5} [18] (2×10^{-6})	$6.7 \times 10^{-7}(\text{tree})$ [17]	6.1×10^{-6} [20] (1×10^{-7})
$ \lambda_{131} \lambda_{132} $	8.2×10^{-5} [18] (2×10^{-6})	$6.7 \times 10^{-7}(\text{tree})$ [17]	7.6×10^{-6} [20] (1×10^{-7})
$ \lambda_{231} \lambda_{232} $	8.2×10^{-5} [18] (2×10^{-6})	4.5×10^{-5}	8.3×10^{-6} [20] (1×10^{-7})

Table 3: *Current (future) constraints on the R-parity violating couplings $LQ\bar{D}$ (see Eq. (2.1)) from LFV processes, assuming that only the listed pair of coupling is nonzero. The current (future) upper limits on the branching ratios are: $\text{Br}(\mu^+ \rightarrow e^+\gamma) < 1.2 \times 10^{-11}$ (10^{-14}), $\text{Br}(\mu^+ \rightarrow e^+e^-e^+) < 1.0 \times 10^{-12}$, and $\text{R}(\mu^- \rightarrow e^- \text{ in Ti}) < 6.1 \times 10^{-13}$ ($\text{R}(\mu^- \rightarrow e^- \text{ in Al}) < 10^{-16}$). Here we assume all the squark masses are degenerate, with $m_{\tilde{q}} = 300 \text{ GeV}$. The notation (tree) indicates that the $\mu^- \rightarrow e^-$ conversion process is generated at the tree-level.*

	$\mu \rightarrow e\gamma$	$\mu \rightarrow eee$	$\mu \rightarrow e \text{ in nuclei}$
$ \lambda'_{111}\lambda'_{211} $	6.8×10^{-4} [18] (2×10^{-5})	1.3×10^{-4}	5.4×10^{-6} (tree) [19] (2×10^{-7})
$ \lambda'_{112}\lambda'_{212} $	6.8×10^{-4} [18] (2×10^{-5})	1.4×10^{-4}	3.9×10^{-7} (tree) [19] (7×10^{-9})
$ \lambda'_{113}\lambda'_{213} $	6.8×10^{-4} [18] (2×10^{-5})	1.6×10^{-4}	3.9×10^{-7} (tree) [19] (7×10^{-9})
$ \lambda'_{121}\lambda'_{221} $	6.8×10^{-4} [18] (2×10^{-5})	2.0×10^{-4}	3.6×10^{-7} (tree) [19] (6×10^{-9})
$ \lambda'_{122}\lambda'_{222} $	6.8×10^{-4} [18] (2×10^{-5})	2.3×10^{-4}	4.3×10^{-5} [20] (7×10^{-7})
$ \lambda'_{123}\lambda'_{223} $	6.9×10^{-4} [18] (2×10^{-5})	2.9×10^{-4}	5.4×10^{-5} [20] (9×10^{-7})

hierarchical neutrinos the bounds on certain products of RPV couplings can be stricter by some orders of magnitude.

When comparing these bounds with the ones from LFV in Tables 2 and 3, we see that for a large number of models the bounds from stopped muon processes are significantly stronger than those from neutrino masses. A proper study of these processes therefore, can shed additional light in the issue of lepton number violation.

References

- [1] Y. Fukuda *et al.* (Super-Kamiokande Collaboration), *Phys. Rev. Lett.* **81** (1998) 1562.
- [2] B.T. Cleveland *et al.*, *Astrophys. J.* **496**(1998) 505; Dzh.N. Abdurashitov *et al.* (SAGE collaboration), *Phys. Rev. Lett.* **77** (1996) 4708; W. Hampe *et al.* (GALLEX Collaboration), *Phys. Lett.* **B447** (1999) 127; Y. Fukuda *et al.* (Super-Kamiokande Collaboration), *Phys. Rev. Lett.* **82** (1999) 1810; *ibid.* **82** (1999) 2430.
- [3] C. Athanassopoulos *et al.* (LSND Collaboration), *Phys. Rev. Lett.* **77** (1996) 3082; *ibid.* **81** (1998) 1774.
- [4] T. Yanagida, in *Proceedings of the Workshop on Unified Theory and Baryon Number of the Universe*, Tsukuba, Japan, 1979, edited by O. Sawada and A. Sugamoto (KEK, Tsukuba, 1979), p. 95; M. Gell-Mann, P. Ramond, and R. Slansky, in *Supergravity*, Proceedings of the Workshop, Stony Brook, New York, 1979, edited by P. van Nieuwenhuizen and D. Freedman (North-Holland, Amsterdam, 1979).
- [5] M. Nakagawa, H. Okonogi, S. Sakata, and A. Toyoda, *Prog. Theor. Phys.* **30** (1963), 727; S. Eliezer and D. Ross, *Phys. Rev.* **D10** (1974) 3088; S.M. Bilenki and B. Pontecorvo, *Phys. Lett.* **61B** (1976) 248; S. Barshay, *Phys. Lett.* **63B** (1976) 466; T.P. Cheng and L.-F. Li in *Proceedings of the Coral Gables Conference*, 1977, ed. A. Perlmutter, Plenum, New York. A. Mann and H. Primakoff, *Phys. Rev.* **D15** (1977) 655; S.T. Petcov, *Yad. Phys.* **25** (1977) 641 and *Sov. J. Nucl. Phys.* **25** (1977) 340; S.M. Bilenki, S.T. Petcov and B. Pontecorvo, *Phys. Lett.* **B67** (1977) 309.

- [6] J. Ellis and D.V. Nanopoulos, *Phys. Lett.* **B110** (1982) 44; R. Barbieri and R. Gatto, *Phys. Lett.* **B110** (1982) 211; G.K. Leontaris, K. Tamvakis and J.D. Vergados, *Phys. Lett.* **B171** (1986) 412; F. Borzumati, and A. Masiero, *Phys. Rev. Lett.* **57** (1986) 961. F. Gabianni and A. Masiero, *Nucl. Phys.* **B322** (1989) 235;
- [7] J. Hisano, T. Moroi, K. Tobe, M. Yamaguchi, and T. Yanagida, *Phys. Lett.* **B357** (1995) 579; J. Hisano, T. Moroi, K. Tobe, and M. Yamaguchi, *Phys. Rev.* **D53** (1996) 2442. K. Tobe, *Nucl. Phys. Proc. Suppl.* **B59** (1997) 223.
- [8] S. Dimopoulos and D. Sutter, *NP B* **452** (1995) 496; B. de Carlos, J.A. Casas and J.M. Moreno, *Phys. Rev.* **D53** (1996) 6398; J. Hisano, D. Nomura, T. Yanagida, *Phys. Lett.* **B437** (1998) 351; J. Hisano and D. Nomura, *Phys. Rev.* **D59** (1999) 116005; M. Gómez, G. Leontaris, S. Lola and J. Vergados, *Phys. Rev.* **D59** (1999) 116009; J. Ellis, M.E. Gomez, G.K. Leontaris, S. Lola, and D.V. Nanopoulos, *Eur. Phys. J.* **C14** (2000) 319; W. Buchmuller, D. Delepine, and F. Vissani, *Phys. Lett.* **B459** (1999) 171; W. Buchmuller, D. Delepine, and L.T. Handoko, *Nucl. Phys.* **B576** (2000) 445; J.L. Feng, Y. Nir and Y. Shadmi, *Phys. Rev.* **D61** (2000) 113005 S. Baek, T. Goto, Y. Okada, and K. Okumura, hep-ph/0002141.
- [9] For a recent review, see Y. Kuno and Y. Okada, hep-ph/9909265.
- [10] L.E. Ibanez, and G.G. Ross, *Nucl. Phys.* **B368** (1992) 3.
- [11] M. Fukugita and T. Yanagida, *Phys. Rev.* **D42** (1990) 1285; B.A. Campbell, S. Davidson, J. Ellis, and K.A. Olive, *Phys. Lett.* **B256** (1991) 457; W. Fischler, G.F. Giudice, R.G. Leigh, and S. Paban, *Phys. Lett.* **B258** (1991) 45.
- [12] For a recent review of baryogenesis at the electroweak scale within supersymmetry see: M. Carena, C.E.M. Wagner, “*Perspectives on Higgs Physics II*”, ed. G.L. Kane, World Scientific, Singapore.
- [13] L. Hall and M. Suzuki, *Nucl. Phys.* **B231** (1984) 419; A.S. Joshipura and M. Nowakowski, *Phys. Rev.* **D51** (1995) 2421; T. Banks, Y. Grossman, E. Nardi, and Y. Nir, *Phys. Rev.* **D52** (1996) 5319; F.M. Borzumati, Y. Grossman, E. Nardi, and Y. Nir, *Phys. Lett.* **B384** (1996) 123; B.

- de Carlos and P.L. White, *Phys. Rev.* **D54** (1996) 3427; A.Yu. Smirnov and F. Vissani, *Nucl. Phys.* **B460** (1996) 37; R. Hempfling, *Nucl. Phys.* **B478** (1996) 3; H.P. Nilles and N. Polonsky, *Nucl. Phys.* **B484** (1997) 33; E. Nardi, *Phys. Rev.* **D55** (1997) 5772; M. Hirsch, H.V. Klapdor-Kleingrothaus, and S.G. Kovalenko, *Phys. Rev.* **D57** (1998) 1947; E.J. Chun, S.K. Kang, C.W. Kim, and U.W. Lee, *Nucl. Phys.* **B544** (1999) 89; O.C.W. Kong, *Mod. Phys. Lett.* **A14** (1999) 903; L. Clavelli and P.H. Frampton, hep-ph/9811326; S. Rakshit and G. Bhattacharyya, and A. Raychaudhuri, *Phys. Rev.* **D59** (1999) 091701; R. Adhikari and G. Omanovic, *Phys. Rev.* **D59** (1999) 073003; D.E. Kaplan and A.E. Nelson, *JHEP* **0001** (2000) 033; A.S. Joshipura and S.K. Vempati, *Phys. Rev.* **D60** (1999) 095009; *ibid* **D60** (1999) 111303; J. Ferrandis, *Phys. Rev.* **D60** (1999) 095012; M. Bisset, O.C.W. Kong, C. Macesanu, and L.H. Orr, *Phys. Rev.* **D62** (2000) 035001; Y. Grossman and H.E. Haber, hep-ph/9906310; A. Abada and M. Losada, hep-ph/9908352, hep-ph/0007041; O. Haug, J.D. Vergados, A. Faessler, and S. Kovalenko, *Nucl. Phys.* **B565** (2000) 38; E.J. Chun and S.K. Kang, *Phys. Rev.* **D61** (2000) 075012; F. Takayama and M. Yamaguchi, *Phys. Lett.* **B476** (2000) 116; R. Kitano and K. Oda, *Phys. Rev.* **D61** (2000) 113001. S. Davidson and M. Losada, *JHEP* **0005** (2000) 021; J.C. Romao, M.A. Diaz, M. Hirsch, W. Porod, and J.W.F. Valle, *Phys. Rev.* **D61** (2000) 071703; hep-ph/0004115.
- [14] M. Nowakowski and A. Pilaftsis, *Nucl. Phys.* **B461** (1996) 19;
- [15] G. Bhattacharyya, H.V. Klapdor-Kleingrothaus and H. Pas, *Phys. Lett.* **B463** (1999) 77.
- [16] S. Lola and G.G. Ross, *Phys. Lett.* **B314** (1993) 336; V. Ben-Hamo, Y. Nir, *Phys. Lett.* **B339** (1994) 77; H. Dreiner and A. Chamseddine, *Nucl. Phys.* **B 458** (1996) 65; P. Binetrui, S. Lavignac and P. Ramond, *Nucl. Phys.* **B477** (1996) 353; G. Bhattacharyya, *Phys. Rev.* **D57** (1998) 3944; P. Binetrui, E. Dudas, S. Lavignac and C.A. Savoy, *Phys. Lett.* **B422** (1998) 171; J. Ellis, S. Lola and G.G. Ross, *Nucl. Phys.* **B526** (1998) 115.
- [17] D. Choudhury and P. Roy, *Phys. Lett.* **B378** (1996) 153.
- [18] M. Chaichian, and K. Huitu, *Phys. Lett.* **B384** (1996) 157.

- [19] J.E. Kim, P. Ko, and D.-G. Lee, *Phys. Rev.* **D56** (1997) 100.
- [20] K. Huitu, J. Maalampi, M. Raidal, and A. Santamaria, *Phys. Lett.* **B430** (1998) 355.
- [21] A. Faessler, T.S. Kosmas, S. Kovalenko, and J.D. Vergados, hep-ph/9904335.
- [22] K. Choi, E.J. Chun, K. Hwang, hep-ph/0005262.
- [23] M. Derrick *et al* (ZEUS Collaboration), *Z. Phys.* **C 73** (1997) 613; C. Adloff *et al.* (H1 Collaboration), *Eur. Phys. J.* **C 11** (1999) 447, err. **C 14** (2000) 553; R. Kerger, hep-ex/0006023, talk at *DIS2000 (8th International Workshop on Deep Inelastic Scattering and QCD)*, Liverpool, 25–30 April 2000; M. Kuze, S. Lola, E. Perez and B.C. Allanach, hep-ph/0007282, summary of *DIS2000*.
- [24] S. Ahmed *et al.*, CLEO Collaboration, *Phys. Rev.* **D61** (2000) 071101
- [25] Y. Kuno and Y. Okada, *Phys. Rev. Lett.* **77** (1996) 434; Y. Kuno, A. Maki, and Y. Okada, *Phys. Rev.* **D55** (1997) 2517.
- [26] S.B. Treiman, F. Wilczek, and A. Zee, *Phys. Rev.* **D16** (1977) 152; A. Zee, *Phys. Rev. Lett.* **55** (1985) 55.
- [27] Y. Okada, K. Okumura, and Y. Shimizu, *Phys. Rev.* **D58** (1998) 051901; *ibid.* **D61** (2000) 094001.
- [28] T. Suzuki, D.F. Measday, and J.P. Roalsvig, *Phys. Rev.* **C35** (1987) 2212.
- [29] H.C. Chiang, E. Oset, T.S. Kosmas, A. Faessler, and J.D. Vergados, *Nucl. Phys.* **A559** (1993) 526; T.S. Kosmas, A. Faessler, F. Simkovic and J.D. Vergados, *Phys. Rev.* **C56** (1997) 526.
- [30] Similar log-enhancements in other models have been discussed. For example, F. Wilczek and A. Zee, *Phys. Rev. Lett.* **38** (1977) 531; W.J. Marciano and A.I. Sanda, *Phys. Rev. Lett.* **38** (1977) 1512; M. Raidal and A. Santamaria, *Phys. Lett.* **B421** (1998) 250.

- [31] L.J. Hall, V.A. Kostelecky, and S. Raby, *Nucl. Phys.* **B 267** (1986) 415; A. E. Faraggi, J.L. Lopez, D.V. Nanopoulos and K. Yuan, *Phys. Lett.* **B221** (1989) 337; S. Kelley, J.L. Lopez, D.V. Nanopoulos and H. Pois, *Nucl. Phys.* **B 358** (1991) 27; R. Barbieri and L.J. Hall, *Phys. Lett.* **B338** (1994) 212; R. Barbieri, L.J. Hall, and A. Strumia, *Nucl. Phys.* **B 445** (1995) 219; A. Ilakovac and A. Pilaftsis, *Nucl. Phys.* **B 437** (1995) 491; P. Ciafaloni, A. Romanino, and A. Strumia, *Nucl. Phys.* **B 458** (1996) 3; N. Arkani-Hamed, H.-C. Cheng, and L.J. Hall, *Phys. Rev.* **D53** (1996) 413; M.E. Gómez and H. Goldberg, *Phys. Rev.* **D53** (1996) 5244; N.G. Deshpande, B. Dutta, and E. Keith, *Phys. Rev.* **D54** (1996) 730 T.V. Duong, B. Butta, and E. Keith, *Phys. Lett.* **B378** (1996) 128 J. Hisano, T. Moroi, K. Tobe, and M. Yamaguchi, *Phys. Lett.* **B391** (1997) 341, erratum **B397** (1997) 357; D. Suematsu, *Phys. Lett.* **B416** (1998) 108 J. Hisano, D. Nomura, Y. Okada, and M. Tanaka, *Phys. Rev.* **D58** (1998) 116010; S.F. King and M. Oliveira, *Phys. Rev.* **D60** (1999) 035003; G. Couture, M. Frank, H. Konig, and M. Pospelov, *Euro. Phys.* **C7** (1999) 139; K. Kurosawa and N. Maekawa, *Prog. Theor. Phys.* **102** (1999) 121; Y. Okada and K. Okumura, *Phys. Rev.* **D61** (2000) 094001; R. Kitano and K. Yamamoto, hep-ph/9905459; G. Barenboim, K. Huitu, and M. Raidal, hep-ph/0005159.
- [32] A. de Gouvêa *et al.*, in preparation.
- [33] L.M. Barkov *et al.*, Research Proposal to PSI, 1999, <http://www.icepp.s.u-tokyo.ac.jp/meg>
- [34] M. Bachman *et al.* (MECO Collaboration), Proposal to BNL, 1997. See also <http://meco.ps.uci.edu>.
- [35] U. Bellgardt, *et al.*, *Nucl. Phys.* **B229** (1988) 1.
- [36] M.L. Brooks, *et al.* (MEGA collaboration), *Phys. Rev. Lett.* **83** (1999) 1521.
- [37] P. Wints (SINDRUM 2 collaboration), 1998 in *Proceedings of the First International Symposium on Lepton and Baryon Number Violation*, ed. H.V. Klapdor-Kleingrothaus and I.V. Krivosheina (Institute of Physics Publishing, Bristol and Philadelphia) p534. See also http://www1.psi.ch/www_sindrum2_hn/sindrum2.html.

- [38] Y. Kuno, presentation at a miniworkshop on Neutrino Factories and Muon Storage Rings at CERN, January 17–19 (2000), <http://muonstoragerings.web.cern.ch/muonstoragerings/>.
See also technical notes in the homepage of the PRISM project <http://psux1.kek.jp/~prism>.